



**COAXIAL WIRE TECHNIQUE: A COMPARISON BETWEEN THEORY  
AND EXPERIMENT**

D. Davino<sup>1,2</sup>, M.R. Masullo<sup>1</sup>, V.G. Vaccaro<sup>1,3</sup>, L. Verolino<sup>1,2</sup>

<sup>1</sup>*INFN-Sezione di Napoli, I-80126 Napoli, Italy*

<sup>2</sup>*Dipartimento di Ingegneria Elettrica, I-80125 Napoli, Italy*

<sup>3</sup>*Dipartimento di Scienze Fisiche I-80126 Napoli, Italy*

**Abstract**

The measurement of the scattering(S) matrix inside the coaxial-wire technique is an entry parameter for the calculation of the coupling impedance of an accelerating machine.

In order to optimize the method of measuring S-matrices we propose, first, a mathematical technique which allows us to know in advance the most precise coefficients of this matrix for a simple and realistic case. Keeping this as reference point we then describe a measuring procedure which gave results in a very good agreement with the theory.

PACS.: 41.20.-q; 11.55.-m; 11.90.+t

*Submitted to Il; Nuovo Cimento B*

*Published by SIS-Pubblicazioni  
Laboratori Nazionali di Frascati*

## 1 INTRODUCTION

Both longitudinal and transverse impedances<sup>1,2,3)</sup> are key parameters for the design of accelerators. Infact, in order not to trigger offensive instabilities, the machine impedances must be kept, with a certain margin, inside the impedance budget. This budget is found by means of stability criteria<sup>4)</sup>, while the margin is chosen according to the reliability of the prediction for the amount of impedance of all machine devices. Among the prediction methods, the one based on bench measurements by means of stretched wire is the most attractive because of its simplicity. This method resort to the measurement of the scattering matrix which, by means of ad hoc manipulations<sup>5)</sup>, gives the value of the device under test (DUT) impedance. We neglect for the moment the discussion and analysis of the procedure which lead from S matrix to the DUT impedance. This argument has been widely treated in the literature<sup>15,16,17)</sup> and it will be the argument of a forthcoming paper.

In this work we want to compare the scattering matrix, theoretically derived, of a simple and realistic device, ohmic losses are included, with the one measured with coaxial wire method. This to the end of improving the measurement techniques mainly in the range of frequencies where the DUT length is comparable or larger than the wavelength. It has to be underlined that, for a reliable comparison, we need also a very precise theoretical tool. The choice of a simple test structure for the measure is due to this end both for experimental reasons and for theoretical approach.

We will, therefore, present and use a new technique for finding the generalized scattering-matrix of a DUT in which a thin wire is stretched on the axis for simulating the bunch passing through. As it is well known, the concept of the generalized scattering-matrix is very closely related to the scattering matrix of circuit theory or of the microwave network theory<sup>6)</sup>. However, it differs from the conventional scattering matrix in that it is extended to consider evanescent as well as propagating modes in the waveguides so that each element of the S-matrix it is an infinite matrix itself. This approach enable us to attack a class of boundary-value problems of guided waves and in particular it is suitable for studying structures in which are present two or more junctions. Their geometry is such that a generalized scattering-matrix description of each of these junctions can be conveniently derived. This enables one to express the solution of the problem in terms of a Neumann series involving matrices of infinite order, the solution being formally exact<sup>8)</sup>.

Recently<sup>7)</sup>, a complete analysis of the coupling between a rectangular waveguide and an open cavity has been developed, considering the relevant eigenfunctions in the waveguide and in the cavity. The mode matching technique proposed here represents an extension of that analysis because the coupling between the feeding waveguide and the cavity is treated in such a way to take into account all the longitudinal modes of the cavity. Infact the factorized form of the field in a cavity can be used to calculate the series related to the longitudinal modes and to obtain an accurate solution by truncating the infinite matrices to a reasonably small size. Furthermore with the MMT we are able to introduce ohmic losses in the test structure in a non perturbative way.

In order to test the technique, we examine a cylindrical pill-box cavity powered by two

coaxial waveguides as shown in Figure 1. We suppose that, except the fundamental mode, a TM electromagnetic field propagates along the waveguides and, as a consequence, in the cavity. In this way we are able to investigate, without loss of generality, a structure useful in accelerator physics, on which a coaxial wire bench measurement can be performed. The scattering matrix is measured by introducing on the DUT axis a small conductive wire on which a current pulse of the same shape of the bunch is riding <sup>5)</sup>.

As a matter of fact these applications need a reliable and effective description of both the resonant modes and the coupling between the cavity and the feeding system.

## 2 REPRESENTATION OF THE FIELD IN THE CAVITY

The electromagnetic field inside a cavity can be expressed in terms of a set of basis functions <sup>9)</sup>

$$\vec{E}(\mathbf{P}) = \sum_i V_i \vec{E}_i(\mathbf{P}), \quad \vec{H}(\mathbf{P}) = \sum_i A_i \vec{H}_i(\mathbf{P}), \quad (2.1)$$

where the coefficients  $V_i$  and  $A_i$  are independent of the coordinates. If the dielectric filling the cavity is homogeneous and isotropic and the expansion functions,  $E_i$ ,  $H_i$ , are orthogonal it can be shown <sup>9)</sup> that the expansion coefficients are given by

$$A_i = \frac{1}{k^2 - k_i^2} \left[ \int_S \hat{\mathbf{n}} \times \vec{E} \vec{H}_i^* dS + k_i \int_S \hat{\mathbf{n}} \times \vec{H} \vec{E}_i^* dS \right] \quad V_i = \frac{-jk_i}{k} \zeta_0 A_i \quad (2.2)$$

where  $S$  is the cavity surface, whose normal versor  $\hat{\mathbf{n}}$  is, as usual, oriented outside the integration domain,  $*$  denotes the complex conjugate,  $k_i$  are the cut-off propagation constants and  $\zeta_0$  is the characteristic impedance of medium filling the waveguide

Due to the symmetry of the structure only TM modes are considered. The rotational symmetry implies the use of two indexes in the expansions (2.1)

$$\vec{E}(r,z) = \sum_{p,s} V_{ps} \vec{E}_{ps}(r,z), \quad \vec{H}(r,z) = \sum_{p,s} A_{ps} \vec{H}_{ps}(r,z), \quad (2.3)$$

where the subscript  $p$  characterises the transverse modes, whereas  $s$  defines the longitudinal ones. For a closed cylindrical cavity of length  $2L$ , it is well known that <sup>9)</sup> the expansion functions assume the factorized form

$$\vec{H}_{ps}(r,z) = \sqrt{\frac{\epsilon_s}{2L}} \Phi_p^c(r) \cos(k_s z) \hat{\phi}, \quad (2.4)$$

where the Neumann's symbol  $\epsilon_s = 1$  if  $s = 0$ ,  $\epsilon_s = 2$  if  $s = 1, 2, 3, \dots$  and  $k_s = \frac{\pi s}{2L}$ ,  $s = 0, 1, 2, \dots$  have been introduced; the transverse modal functions  $\Phi_p^c(r)$  are related to transverse eigenvalues (the apex  $c$  stays for cavity) and have the functional form<sup>1</sup> for a coaxial guide with  $c$  and  $a$  respectively outer and inner radii :

---

<sup>1</sup> The subscript 1 indicates the fundamental mode, whereas  $p = 2, 3, \dots$  indicates the higher order modes.

$$\Phi_p^c(r) = \begin{cases} \frac{1}{r\sqrt{2\pi \ln(c/a)}} & p = 1, \\ \frac{x_p\sqrt{\pi}}{2a} \frac{J_1(rx_p/a)Y_0(x_p) - J_0(x_p)Y_1(rx_p/a)}{\sqrt{J_0^2(x_p)/J_0^2(cx_p/a) - 1}} & p = 2, 3, \dots, \end{cases} \quad (2.5)$$

The cut-off propagation constants are given as

$$k_{ps}^2 = \left(\frac{x_p}{a}\right)^2 + k_s^2 \quad (2.6)$$

and  $x_p$  is the  $p$ -th solution of the equation

$$x [J_0(\alpha x)Y_0(x) - J_0(x)Y_0(\alpha x)] = 0, \quad (2.7)$$

with  $\alpha = c/a$ . Moreover the expansion coefficients assume the simplified form <sup>9)</sup>

$$\zeta_0 A_{ps} = \frac{j\mathbf{k}}{k^2 - k_{ps}^2} \oint_S \hat{\mathbf{n}} \times \vec{\mathbf{E}} \vec{\mathbf{H}}_{ps}^* dS, \quad V_{ps} = -\frac{j\mathbf{k}_{ps}}{k} \zeta_0 A_{ps}. \quad (2.8)$$

Note explicitly that the tangential electric field appearing in equation (2.8) is the actual field over  $S$ . It is not given by the first of expressions (2.3), which, differently from the expression for the tangential magnetic field, does not provide a representation for the tangential component uniformly valid up to cavity boundaries.

### 3 REPRESENTATION OF THE FIELD IN THE WAVEGUIDES

It is well known that the study of the electromagnetic field inside a propagating structure can be performed by a separation of the electromagnetic field according to the longitudinal (along  $z$ ) and transverse components (the subscript  $t$  stays for transverse) <sup>9,10)</sup>

$$\vec{\mathbf{E}}(\mathbf{P}) = \vec{\mathbf{E}}_t(\mathbf{P}) + E_z(\mathbf{P}) \hat{\mathbf{z}}, \quad \vec{\mathbf{H}}(\mathbf{P}) = \vec{\mathbf{H}}_t(\mathbf{P}) + H_z(\mathbf{P}) \hat{\mathbf{z}}. \quad (3.1)$$

Introducing a polar system of coordinates  $(r, \varphi)$  in the transverse section and referring to TM modes ( $H_z = 0$ ), we can write the electromagnetic field by means of the following modal expansion

$$\begin{aligned} \vec{\mathbf{E}}_t(\mathbf{P}) &= \sum_n V_n(z) \vec{\mathbf{e}}_n(r, \varphi) & E_z(\mathbf{P}) &= \frac{\zeta_0}{j\mathbf{k}} \sum_n k_n A_n(z) \Phi_n(r, \varphi) \\ \vec{\mathbf{H}}_t(\mathbf{P}) &= \sum_n A_n(z) \vec{\mathbf{h}}_n(r, \varphi) & H_z(\mathbf{P}) &= 0, \end{aligned} \quad (3.2)$$

where  $\vec{\mathbf{e}}_n(r, \varphi)$  and  $\vec{\mathbf{h}}_n(r, \varphi)$  are the vector mode functions, whereas  $V_n(z)$  and  $A_n(z)$  are the scalar ones,  $k_n$  is the transverse eigenvalue,  $k$  is the propagation constant <sup>9,10)</sup>. The scalar mode functions have to obey the ‘telegraphers’ equations and therefore the transverse fields can be rewritten <sup>9,10)</sup> as

$$\vec{E}_t(\mathbf{P}) = \sum_n [V_n^+(z) + V_n^-(z)] \vec{e}_n(r, \varphi), \quad \vec{H}_t(\mathbf{P}) = \frac{1}{\zeta_0} \sum_n \frac{V_n^+(z) - V_n^-(z)}{\zeta_n^w} \vec{h}_n(r, \varphi), \quad (3.3)$$

namely as a superposition of a forward wave  $V_n^+(z)$  and of a backward one  $V_n^-(z)$ ; the modal impedance  $\zeta_n^w$  is given by

$$\zeta_n^w = \frac{\sqrt{(ka)^2 - w_n^2}}{ka} \quad w_n \leq ka, \quad \zeta_n^w = -j \frac{\sqrt{w_n^2 - (ka)^2}}{ka} \quad w_n \geq ka, \quad (3.4)$$

where the apex  $w$  stays for waveguide and  $w_n$  are real zeros of the equation

$$x [J_0(\alpha x) Y_0(x) - J_0(x) Y_0(\alpha x)] = 0, \quad \text{with} \quad \alpha = b/a. \quad (3.5)$$

with  $a$  the inner waveguide radius and  $b$  the outer one.

For simplifying the mathematical treatment of the problem, we examine an axial symmetric case, so the functional dependence by  $\phi$  will be omitted in the following. As a consequence, using the property of the vector mode orthogonality for  $\vec{e}_n$  and  $\vec{h}_m$  one can evaluate these functions for a coaxial cable <sup>10)</sup>

$$\vec{e}_m(r) = \hat{r} \Phi_m^w(r), \quad \vec{h}_m(r) = \hat{\phi} \Phi_m^w(r), \quad (3.6)$$

where  $\Phi_m^w(r)$  is the linear combinations of Bessel functions

$$\Phi_m^w(r) = \begin{cases} \frac{1}{r\sqrt{2\pi \ln(b/a)}} & m = 1, \\ \frac{w_m \sqrt{\pi}}{2a} \frac{J_1(rw_m/a) Y_0(w_m) - J_0(w_m) Y_1(rw_m/a)}{\sqrt{J_0^2(w_m)/J_0^2(bw_m/a) - 1}} & m = 2, 3, \dots \end{cases} \quad (3.7)$$

Let us finally note that the expression (3.7) for the waveguide is similar to the equation (2.5) for the cavity.

#### 4 WAVEGUIDE-CAVITY COUPLING

In the above field expression, equ. (2.8) and (3.3), the coefficients  $A_{ps}$  and  $V_n^\pm$  are unknown quantities, which can be resolved by imposing the field matching, namely the continuity of the tangential component of the magnetic and electric field on the coupling apertures,  $S_1$  ( $z = 0$  and  $a \leq r \leq b$ ) and  $S_2$  ( $z = 2L$  and  $a \leq r \leq b$ ). This cannot be explicitly done for the tangential component of the electric component because of the non-uniform convergence of the first expansion (2.3) on the cavity boundaries: the tangential component of the electric field in the cavity vanishes on the boundaries. Instead the continuity of the tangential component of the magnetic field over the coupling aperture  $S_1$  ( $z = 0$  and  $a \leq r \leq b$ ) gives

$$\sum_{p,s} \sqrt{\frac{\epsilon_s}{2L}} A_{ps} \Phi_p^c(r) = \frac{1}{\zeta_0} \sum_q \frac{V_{1q}^+ - V_{1q}^-}{\zeta_q^w} \Phi_q^w(r), \quad r \in S_1, \quad (4.1)$$

where expansion (3.3) of the tangential component of the magnetic field in the waveguide, and representation (2.3) of the magnetic field in the cavity have been used. We put for

brevity  $V_q^+(0) = V_{1q}^+$  and  $V_q^-(0) = V_{1q}^-$ . Similarly the matching over the aperture  $S_2$  ( $z = 2L$  and  $a \leq r \leq b$ ) gives

$$\sum_{p,s} (-1)^s \sqrt{\frac{\epsilon_s}{2L}} A_{ps} \Phi_p^c(r) = -\frac{1}{\zeta_0} \sum \frac{V_{2q}^+ - V_{2q}^-}{\zeta_q^w} \Phi_q^w(r), \quad r \in S_2, \quad (4.2)$$

where  $V_q^+(2L) = V_{2q}^+$  and  $V_q^-(2L) = V_{2q}^-$ . Both relations (4.1) and (4.2) are valid for  $a \leq r \leq b$ ; so we can project them on the complete set of the modes of the coaxial cable  $\Phi_q^w(r)$ , obtaining the following system of equations

$$Y_q^w (V_{1q}^+ - V_{1q}^-) = \zeta_0 \sum_{p=1}^{\infty} C_{pq} \sum_{s=0}^{\infty} \sqrt{\frac{\epsilon_s}{2L}} A_{ps} = \zeta_0 \sum_{p=1}^{\infty} C_{pq} (A_p^E + A_p^O) \quad (4.3)$$

$$Y_q^w (V_{2q}^- - V_{2q}^+) = \zeta_0 \sum_{p=1}^{\infty} C_{pq} \sum_{s=0}^{\infty} (-1)^s \sqrt{\frac{\epsilon_s}{2L}} A_{ps} = \zeta_0 \sum_{p=1}^{\infty} C_{pq} (A_p^E - A_p^O) \quad (4.4)$$

where the coefficients  $C_{pq}$  defined and evaluated in the appendix A take into account the coupling among the waveguide and the cavity modes and  $Y_w = \text{diag} [\zeta_p^w]^{-1}$ . Furthermore the two series  $A_p^E$  and  $A_p^O$  defined in equations (4.3) and (4.4) can be expressed in a closed form.

In order to investigate the electromagnetic coupling between the waveguides and the cavity, we have to evaluate the expansion coefficients  $A_{ps}$  given by the integrals (2.8) and therefore to know the electric field on the cavity surfaces. If we assume that both the cavity and the waveguides are perfectly conducting, the contribution to the coefficient value (2.8) comes only from the coupling apertures, that is

$$\zeta_0 A_{ps} = \frac{jk}{k^2 - k_{ps}^2} \int_{S_1+S_2} \hat{n} \times \vec{E} \vec{H}_{ps}^* dS. \quad (4.5)$$

As already noted above, the tangential component of the electric field cannot be obtained on the cavity boundary by means of the representation (2.3). This difficulty can be overcome by the modal expansion (3.3) and because of the continuity of the tangential component of the electric field it is

$$\zeta_0 A_{ps} = \frac{jk}{k^2 - k_{ps}^2} \sqrt{\frac{\epsilon_s}{2L}} \sum_{t=1}^{\infty} [(-1)^s (V_{2t}^+ + V_{2t}^-) - V_{1t}^+ - V_{1t}^-] C_{pt} \quad (4.6)$$

where, as before, the coefficients  $C_{pt}$  are in the Appendix A. The relation (4.6) delineates an explicit dependence from the index  $s$  of the coefficients  $A_{ps}$ . This fact implies that we are able to get for the two series appearing in (4.3) and (4.4) the following expressions <sup>11)</sup>

$$A_p^E = j \frac{\cotg(kL \zeta_p^c)}{2 \zeta_0 \zeta_p^c} \sum_{t=1}^{\infty} [V_{2t}^+ + V_{2t}^- - V_{1t}^+ - V_{1t}^-] C_{pt} \quad (4.7)$$

$$A_p^O = j \frac{\text{tg}(kL \zeta_p^c)}{2 \zeta_0 \zeta_p^c} \sum_{t=1}^{\infty} [V_{2t}^+ + V_{2t}^- + V_{1t}^+ + V_{1t}^-] C_{pt} \quad (4.8)$$

In this way, from a physical point of view, we have taken into account all the longitudinal modes of the cavity. Substituting the sums (4.7) and (4.8) into relations (4.3) and (4.4) respectively, we get a system containing only the powering waves

$$\begin{cases} (\mathbf{Y}_w + \mathbf{O} - \mathbf{E}) \mathbf{V}_1^- + (\mathbf{O} + \mathbf{E}) \mathbf{V}_2^- = (\mathbf{Y}_w - \mathbf{O} + \mathbf{E}) \mathbf{V}_1^+ - (\mathbf{O} + \mathbf{E}) \mathbf{V}_2^+ \\ (\mathbf{O} + \mathbf{E}) \mathbf{V}_1^- + (\mathbf{Y}_w + \mathbf{O} - \mathbf{E}) \mathbf{V}_2^- = -(\mathbf{O} + \mathbf{E}) \mathbf{V}_1^+ + (\mathbf{Y}_w - \mathbf{O} + \mathbf{E}) \mathbf{V}_2^+ \end{cases} \quad (4.9)$$

where for the sake of simplicity we called

$$\mathbf{E} = \frac{j}{2} \mathbf{C}^T \mathbf{Y}_c \cotg(kL\mathbf{Z}_c) \mathbf{C} \quad \mathbf{O} = \frac{j}{2} \mathbf{C}^T \mathbf{Y}_c \tg(kL\mathbf{Z}_c) \mathbf{C} \quad (4.10)$$

and we defined the following matrices and vectors

$$\mathbf{C} = [\mathbf{C}_{pq}], \quad \mathbf{Y}_w = \text{diag} [\zeta_p^w]^{-1}, \quad \mathbf{Z}_c = \text{diag} [\zeta_p^c], \quad \mathbf{V}_m^\pm = [\mathbf{V}_{mp}^\pm, m=1, 2], \quad \mathbf{Y}_c = \mathbf{Z}_c^{-1}$$

Before going on we have to point out some features of our formulation. In eqs. (4.9) the resonant behaviour of the cavity appears straightforward and it is included in the two terms  $\mathbf{O}$  and  $\mathbf{E}$ :  $\mathbf{Y}_c$  goes to infinity in the case of transverse resonances, meanwhile the cotangent (tangent) terms go to infinity for the longitudinal ones. Our use of field expansions in normal modes has brought us to the useful series (4.7) and (4.8) containing the resonant cavity modes and leading to closed forms.

Furthermore, the term  $\mathbf{Y}_w$  contains all the information on the waveguides behaviour.

## 5 SCATTERING MATRIX

We are now ready to evaluate the generalized scattering matrix. Taking into account that our device under test is symmetric ( $S_{11}=S_{22}$ ) and reciprocal ( $S_{12}=S_{21}$ ), we have to compute only  $S_{11}$  e  $S_{12}$ .

We start by getting the difference  $\mathbf{V}_1^- - \mathbf{V}_2^-$ , and the sum  $\mathbf{V}_1^- + \mathbf{V}_2^-$  from the system (4.9), obtaining

$$\begin{cases} \mathbf{V}_1^- - \mathbf{V}_2^- = (\mathbf{A} - \mathbf{E})^{-1} (\mathbf{A} + \mathbf{E}) (\mathbf{V}_1^+ - \mathbf{V}_2^+) \\ \mathbf{V}_1^- + \mathbf{V}_2^- = (\mathbf{A} + \mathbf{O})^{-1} (\mathbf{A} - \mathbf{O}) (\mathbf{V}_1^+ + \mathbf{V}_2^+) \end{cases} \quad (5.1)$$

As a consequence, it is simple to define the generalized scattering matrix

$$\begin{cases} \mathbf{V}_1^- = \mathbf{S}_{11} \mathbf{V}_1^+ + \mathbf{S}_{12} \mathbf{V}_2^+ \\ \mathbf{V}_2^- = \mathbf{S}_{21} \mathbf{V}_1^+ + \mathbf{S}_{22} \mathbf{V}_2^+ \end{cases} \quad (5.2)$$

where the reflection matrix is defined by

$$\mathbf{S}_{11} = \mathbf{S}_{22} = \frac{1}{2} [(\mathbf{A} + \mathbf{O})^{-1} (\mathbf{A} - \mathbf{O}) + (\mathbf{A} - \mathbf{E})^{-1} (\mathbf{A} + \mathbf{E})] \quad (5.3)$$

and the transmission matrix is given by

$$\mathbf{S}_{12} = \mathbf{S}_{21} = \frac{1}{2} [(\mathbf{A} + \mathbf{O})^{-1} (\mathbf{A} - \mathbf{O}) - (\mathbf{A} - \mathbf{E})^{-1} (\mathbf{A} + \mathbf{E})] \quad (5.4)$$

It is obvious that the reflection (5.3) and the transmission (5.4) matrices are of infinite dimension. In practice, the order of these matrices depends upon the modes propagating through the structure. Performing a numerical elaboration, one has to truncate these matrices to a finite dimension (N), which indicates how many transverse modes propagate in the structure. This dimension is related to the maximum working frequency and goes up on increasing this frequency. We have verified by means of numerical experiments hereafter proposed that in practical cases only a few modes are useful to describe the propagation in our structure.

Nevertheless we verified, by numerical experiments, that the inversion procedure of the truncate matrices is well behaved and stable: we shall say that a Nth order inverse has been found if the elements of an Nth order matrix formed by truncating the inverse matrix of an (N+M)th order solution does not change appreciably as M increased.

Finally we observe that if only the fundamental mode propagates in the waveguide ( $w_1 = 0$ ) and in the cavity ( $c_1 = 0$ ), the previous formulae can be simplified, and the reflection and transmission matrices becomes the scalar quantities, given by

$$S_{11}(1,1) = \frac{1}{2} \left[ \frac{1 - j\alpha \operatorname{tg}(kL)}{1 + j\alpha \operatorname{tg}(kL)} + \frac{1 + j\alpha \operatorname{cotg}(kL)}{1 - j\alpha \operatorname{cotg}(kL)} \right], \quad S_{12}(1,1) = \frac{1}{2} \left[ \frac{1 - j\alpha \operatorname{tg}(kL)}{1 + j\alpha \operatorname{tg}(kL)} - \frac{1 + j\alpha \operatorname{cotg}(kL)}{1 - j\alpha \operatorname{cotg}(kL)} \right],$$

where  $\alpha = \ln(b/a)/\ln(c/a)$ .

## 6. OHMIC LOSSES

Till now we have considered the contribution to the integral in eq. (2.8) due to the coupling apertures only, because the other terms are null for a perfect conducting material. If we want to complete the study of the electromagnetic coupling between the waveguide and the cavity, ohmic losses are to be introduced in the cavity walls: the tangential component of the electric field will be no more vanishing there and one can evaluate the expansion coefficient (2.8) also on the cavity surfaces. The definition of these coefficients needs the knowledge of the electric field on the cavity surface. The Leontovič boundary condition<sup>9,10)</sup>

$$\hat{n} \times \vec{E} = \frac{1+j}{\sigma\delta} \hat{n} \times (\vec{H} \times \hat{n}) = \frac{1+j}{\sigma\delta} \vec{H}_t \quad (6.1)$$

wherein  $\sigma$  is the electric conductivity of the metallic regions and  $\delta = \sqrt{2/(\omega\mu\sigma)}$  is the penetration depth, can be used to express the (tangential) electric field over the metallic surfaces in terms of the magnetic field, given by expressions (2.3). In this case we include ohmic losses in a non perturbative way. The ohmic losses change the cavity eigenvalues, acting as a sort of source diffused on the cavity walls.

Regarding the coefficients  $A_{ps}$ , we note that they depend on the electric field and on

the inner cavity surface  $S$ . The integral can be evaluated by dividing the surface  $S$  according to the following sub-domains :

- the lateral surface  $S_c$  of the cavity ( $r=c$  and  $0 \leq z \leq 2L$ );
- the surrounding surface  $S_a$  of the wire ( $r=a$  and  $0 \leq z \leq 2L$ );
- the lateral surfaces of the cavity  $B_1$  ( $z=0$  and  $b \leq r \leq c$ ) and  $B_2$  ( $z=2L$  and  $b \leq r \leq c$ ).

Following the geometrical scheme listed above, the integration (2.8) can be considered as the superposition of four contributions where the first one is related to the coupling through the apertures and has been discussed in the previous section. The other ones will be discussed and evaluated below, using Leontovič condition (6.1) for the different cases.

- All along the lateral surface  $S_c$  of the cavity [ $\hat{n} = \hat{r}$ ] we get

$$\iint_{S_c} \hat{r} \times \vec{E}(P) \vec{H}_{ps}^*(P) dS = \zeta 2\pi c \sum_{m,q} A_{mq} \int_0^{2L} \vec{H}_{mq}(c,z) \vec{H}_{ps}^*(c,z) dz .$$

where  $\zeta = \frac{1+j}{\sigma\delta}$  is the surface impedance.

Performing the trivial integration on  $z$  <sup>11)</sup>, we finally have

$$\iint_{S_c} \hat{r} \times \vec{E}(P) \vec{H}_{ps}^*(P) dS = \zeta 2\pi c \vec{h}_p^c(c) \sum_m A_{ms} \vec{h}_m^c(c) . \quad (6.2)$$

- Repeating the same considerations along the surrounding surface  $S_a$  of the wire [ $\hat{n} = -\hat{r}$ ], we obtain

$$\iint_{S_a} \hat{r} \times \vec{E}(P) \vec{H}_{ps}^*(P) dS = \zeta 2\pi a \vec{h}_p^c(a) \sum_m A_{ms} \vec{h}_m^c(a) . \quad (6.3)$$

Summing relations (6.2) and (6.3) we get

$$\iint_{S_a+S_c} \hat{r} \times \vec{E}(P) \vec{H}_{ps}^*(P) dS = \zeta \sum_m L_{pm} I_m(s) , \quad (6.4)$$

where the generic element of the matrix  $\mathbf{L} = \{L_{pm}\}$  is given by

$$L_{pm} = 2\pi \left[ c \vec{h}_p^c(c) \vec{h}_m^c(c) + a \vec{h}_p^c(a) \vec{h}_m^c(a) \right] . \quad (6.5)$$

- The contribution of the two lateral surfaces of the cavity  $B_1$  (where  $\hat{n} = -\hat{z}$ ) and  $B_2$  (where  $\hat{n} = \hat{z}$ ) can be computed using the modal expansion of the fields (A.3) and the Leontovič condition (5.1) again, namely

$$\iint_{B_1+B_2} \hat{n} \times \vec{E}(P) \vec{H}_{ps}^*(P) dS = \zeta \sum_{m,q} A_{mq} \frac{\sqrt{\epsilon_q \epsilon_s}}{2L} [1 + (-1)^{s+q}] B_{pm} , \quad (6.6)$$

where the symmetric matrix  $\mathbf{B} = \{B_{nm}\}$  is defined and evaluated in the Appendix B. Summarising the previous results and representing the symmetric matrix <sup>12)</sup>

$$\text{diag}[(k_p)^2] + j \frac{\zeta}{\zeta_0} k \mathbf{L} = \mathbf{U} \mathbf{D} \mathbf{U}^{-1}, \quad (6.7)$$

by means of the eigenvalue diagonal matrix,  $\mathbf{D} = \text{diag}(\lambda_p^2)$ , which corresponds to the eigenvector matrix  $\mathbf{U} = \{U_{pm}\}$ , the elements of the scattering matrix can be written in forms similar to eqs. (5.3) and (5.4), following the same scheme outlined in the previous section; new matrices have to be defined that take into account the losses

$$\begin{aligned} \mathbf{E} &= \frac{j}{2} \mathbf{C}^T \left[ \mathbf{U} \mathbf{Z}_c \text{tg}(kL\mathbf{Z}_c) \mathbf{U}^{-1} + j \frac{\zeta}{\zeta_0} \mathbf{B} \right]^{-1} \mathbf{C}, \\ \mathbf{O} &= \frac{j}{2} \mathbf{C}^T \left[ \mathbf{U} \mathbf{Z}_c \text{cotg}(kL\mathbf{Z}_c) \mathbf{U}^{-1} - j \frac{\zeta}{\zeta_0} \mathbf{B} \right]^{-1} \mathbf{C}, \\ \mathbf{Z}_c &= \text{diag} \left[ \frac{\sqrt{k^2 - \lambda_p^2}}{k} \right]. \end{aligned} \quad (6.8)$$

It is worth noting that these new matrices (6.8) give again the old ones (4.10) in the case  $\sigma = \infty$  (perfectly conducting case) and the eigenvalues  $\lambda_p$  fall back in the transverse eigenvalues  $k_p$ . The ohmic losses change the cavity eigenvalues, acting as a sort of source diffused on the cavity walls. It has to be noticed that, in this way, the coefficients  $A_{ps}$  contain all the information regarding the losses and the apertures.

## 7 NUMERICAL RESULTS AND APPROXIMATIONS

We started the numerical experiments with a cavity defined by the following inner and outer diameter, length and external waveguide diameter

$$2a = 0.75 \text{ mm} \quad 2c = 25.7 \text{ cm} \quad 2L = 38.7 \text{ cm} \quad 2b = 6.87 \text{ cm} ;$$

with all the metallic regions exhibiting an electrical conductivity  $\sigma = 58 \text{ MS/m}$ .

We decided to examine the spectrum of some elements of the scattering matrix up to 4 GHz. Therefore we studied the convergence of the proposed method around the 1 GHz and the maximum working frequency in order to estimate the minimum order of the scattering matrix. The procedure establishes with a very small dimension of the matrix ( $N \approx 8$ ), as the Figure 2 distinctly indicates. This implies that we are able to examine the transmission element  $S_{12}(1,1)$  up to 4 GHz with high accuracy by inverting a matrix of dimension four. Similarly around a resonance frequency for  $S_{12}(1,1)$ , Figure 3 shows that 10 elements establish the numerical evaluations with a good accuracy.

## 8 EXPERIMENTAL RESULTS AND COMPARISON

The coaxial wire method<sup>13,14,15,16)</sup> is a well known technique used to characterize electromagnetic structures, which have to be inserted in particle accelerators, by measuring

their transmission scattering matrix. The Device Under Test is transformed in a coaxial structure by introducing a wire on its longitudinal axis.

In (Ref.5) a general relationship between the scattering matrix and the coupling impedance is given in which the  $S_{12}$  coefficient is calculated as referred to the DUT characteristic impedance and not to the external measurement apparatus and with no approximation in the formula.

Even if this method is usually used to evaluate the unknown coupling impedance of a bunch travelling the same structure, some care has to be taken in the result evaluation, because the wire presence modifies the electromagnetic field behaviour. The validity of the coaxial wire method has been investigated in some cases <sup>17)</sup>.

In order to look for an experimental validation of the MMT we apply the method to the cavity shown in figure 1 using a wire of 0.375 mm radius. In particular we perform our measurements in the frequency domain <sup>16,18)</sup>, acquiring the transmission scattering matrix of the device (DUT) and of a reference line (REF), which has the same length as the cavity and radius equal to the small aperture shown in Fig. 1. The simulation runs have been performed on a cavity with the same geometry of measured one.

A Network Analyzer Hp 8720C (50MHz – 13.5 GHz) has been used for the measurements in the range 0-4 GHz . The Network gives directly in output the scattering parameters. A Power-Mac is connected through a HP-IP bus to the instrumentation for its control and for the acquisition of the data, real and imaginary parts of the  $S_{ij}$  parameters (Labview enviroment). An accurate calibration has been performed for the entire band of acquisition including all the cables and the connectors.

Both the REF and the DUT structures have geometrical and electrical impedance adapters in order to minimize the reflections and to improve the signal to noise ratio. Because some resonances could be really small and because we want well characterize the sample structure, we need a "clean" signal. For this reason the adaptor system, mechanical and electrical, has to be carefully setted up.

The wire thickness of 0.75 mm was for us a good "compromise" between the possibility of acquire a good signal and the modification of the bunch case e.m. field distribution.with respect to the wire case.

Figure. (4) shows the comparison between the experimental data and the simulations performed in the same range of frequencies The agreement is really good also for some small resonances. Longitudinal and transverse resonances could be recognized varying some geometrical parameters in the simulations.

In order to better understand the quality of the agreement, level and frequency values, we studied some resonances in particular, 1st and 4th. In fig. (5) the comparison is reported between the simulation and experimental data, different runs have been performed changing the waveguide radius. Again the agreement is satisfactory also because we can recognize the same frequencies value and the same pick level. The comparison on the resonances level gives us a tool to understand how precise the measure is.

## 9 CONCLUSIONS AND PERSPECTIVES

The analysis of the coupling between a feeding coaxial cable and a coaxial circular cavity has been developed by taking into account all the modes in the cable and in the cavity. An explicit formula has been obtained for the scattering matrix, which provides a simple and accurate tool for studying the coupling, and for allowing the design of such a structure without using a cumbersome numerical analysis.

Finally, the comparison with the experimental results has shown both the reliability of the implemented theoretical tool and the possibility to perform very precise bench measurements of the scattering matrix. At the same time we got a good starting point for the understanding of all the existing differences between impedance measurements with the bunch and with the coaxial wire method.

## 10 REFERENCES

- (1) Heifets S.A., Kheifets S.A., Coupling impedance in modern accelerators, *Review of Modern Physics*, **63**(3), (July 1991).
- (2) Palumbo L., Vaccaro V.G., Zobov M., Wake fields and impedance, LNF-94/041 (P), 5 September 1994; CERN 95-06 report of the CAS, pp. 331, (November 1995).
- (3) Vaccaro V.G., CERN ISR-RF/66-35 (1966).
- (4) A.W. Chao, SLAC PUB-2946 (1982)
- A.W. Chao, *Physics of Collective Beam Instabilities in High Energy Accelerators*, Wiley series in Beam Physics and Accelerator Technology, NY
- (5) Vaccaro V.G., Coupling measurements: an improved wire method, INFN/TC-94/023 (1994).
- (6) Collin R.E., *Foundations for microwave engineering*, (McGraw-Hill 1992).
- (7) Bucci O.M., Di Massa G., Open resonators powered by a rectangular waveguide, *IEE Proceedings-II* **139**(4), (August 1992).
- (8) Lee S.W., Mittra R., *Analytical techniques in the theory of guided waves*, (The Macmillan Company, New York 1971).
- (9) Franceschetti G., *Campi elettromagnetici*, (Boringhieri, Torino 1983).
- (10) Marcuvitz N., *Waveguide handbook*, (IEE Electromagnetic waves series, New York 1950).
- (11) Gradshteyn I.S., Ryzhik I.M., *Table of integrals, series, and products*, (Academic Press 1980).
- (12) Gantmacher F.M., *Applications of the theory of matrices*, Wiley, New York, (1959).
- (13) M. Sands and J.R. Rees, A bench measurement of the energy loss of a stored beam to a cavity, SLAC report PEP-0095 (1975).
- (14) H.Hahn and F.Pederson, Brookhaven National Laboratory report BNL-50870 (April 1978)
- (15) L.S. Walling, D.E. Mc Murry, D.V. Neuffer and H.A. Thiessen, Transmission-line impedance measurements for an advanced hadron facility, *NIM in Physic Research* **A281**, pp. 433-447,(1989)
- (16) F.Galluccio, M.R. Masullo, V.G.Vaccaro, B.Schwingenheuer, F.Klefenz, R.Wanzenberg and M.Wendt, Measurement of the longitudinal couplig impedance of the Hera-B vertex detector chamber, *Proceedings of the V EPAC, Sitges (Barcellona)*, pp. 1356.(1996)
- (17) Gluckstern R.L., Li R., Analysis of coaxial measurements of longitudinal coupling impedance, *Particle Accelerators*, **29**, pp. 159-165, (1990).
- (18) D.Davino, L.Verolino, M.R.Masullo and V.G. Vaccaro, Mode matching technique for a lossy pill-box cavity, *Proc. of the VI EPAC, Stockholm*, pp. 1359 (June 1998).

## Appendix A

Aim of this appendix is to discuss the evaluation and some properties of the coefficients

$$C_{pq} = \int_A \Phi_p^c(r) \Phi_q^w(r) dS = 2\pi \int_a^b \Phi_p^c(r) \Phi_q^w(r) r dr, \quad (\text{A.1})$$

which take into account the coupling due the apertures among the modes of the waveguide and of the cavity. Using the remarkable integral [RG]

$$(\alpha^2 - \beta^2) \int_0^r x Z_p(\alpha x) B_p(\beta x) dx = \beta r Z_p(\alpha r) B_{p-1}(\beta r) - \alpha r Z_{p-1}(\alpha r) B_p(\beta r) \quad (\text{A.2})$$

where  $Z_p(x)$  e  $B_p(x)$  are linear combination of Bessel functions, we have ( $p, q \geq 2$ )

$$C_{pq} = \frac{\pi c_p^2 J_0(w_q) / J_0(bw_q/a)}{\sqrt{J_0^2(w_q)/J_0^2(bw_q/a) - 1} \sqrt{J_0^2(x_p)/J_0^2(cx_p/a) - 1}} \frac{J_0(bx_p/a) Y_0(x_p) - Y_0(bx_p/a) J_0(x_p)}{w_q^2 - x_p^2} \quad (\text{A.3})$$

where  $w_q$  and  $x_p$  are the transverse eigenvalues of the waveguide and of the cavity respectively, namely they are solution of the equation (2.7) with  $\alpha = b/a$  and  $\alpha = c/a$ .

The elements of the first row and the first column of the matrix  $\mathbf{C}$  are related to the fundamental mode (TEM). We get for the first row and the first column

$$C_{1q} = \sqrt{\frac{2\pi}{\ln(c/a)}} \int_a^b \Phi_q^w(r) dr = 0 \quad \text{for } q = 2, 3, 4, \dots, \quad (\text{A.4})$$

$$C_{p1} = \sqrt{\frac{2\pi}{\ln(b/a)}} \int_a^b \Phi_p^c(r) dr = \pi \frac{J_0(x_p) Y_0(bx_p/a) - J_0(bx_p/a) Y_0(x_p)}{\sqrt{2 \ln(b/a)} \sqrt{J_0^2(c_p)/J_0^2(cx_p/a) - 1}} \quad \text{for } p = 2, 3, 4 \dots (\text{A.5})$$

Finally  $C_{11}$  is given by

$$C_{11} = \frac{1}{\sqrt{\ln(b/a) \ln(c/a)}} \int_a^b \frac{dr}{r} = \sqrt{\frac{\ln(b/a)}{\ln(c/a)}}. \quad (\text{A.6})$$

## Appendix B

In this appendix we perform the evaluation of the coefficients  $B_{nm}$

$$B_{nm} = \iint_B \Phi_n^c(r) \Phi_m^c(r) dS = 2\pi \int_b^c \Phi_n^c(r) \Phi_m^c(r) r dr . \quad (\text{B.1})$$

From the definition it follows immediately that is the matrix  $\mathbf{B}$  is symmetric. Thus, starting with the first element  $B_{11}$ , it is

$$B_{11} = \frac{1}{\ln(c/a)} \int_b^c \frac{dr}{r} = \frac{\ln(c/b)}{\ln(c/a)} . \quad (\text{B.2})$$

We continue with the other elements of the first row (the first column) <sup>11)</sup>

$$B_{1m} = \sqrt{\frac{2\pi}{\ln(c/a)}} \int_b^c \Phi_m^c(r) dr = \pi \frac{J_0(bc_m/a) Y_0(c_m) - J_0(c_m) Y_0(bc_m/a)}{\sqrt{2 \ln(c/a)} \sqrt{J_0^2(c_m)/J_0^2(cc_m/a) - 1}} . \quad (\text{B.3})$$

and the other off-diagonal elements, using the integral (A.2), are

$$B_{nm} = \sqrt{2\pi \ln(c/a)} b \frac{c_n^2 B_{1n} \Phi_m^c(b) - c_m^2 B_{1m} \Phi_n^c(b)}{c_n^2 - c_m^2} \quad (\text{B.4})$$

The elements of the main diagonal can be obtained from the last relation in the limit  $c_n \rightarrow c_m$ , namely

$$B_{nn} = \sqrt{2\pi \ln(c/a)} b B_{1n} \Phi_n^c(b) .$$

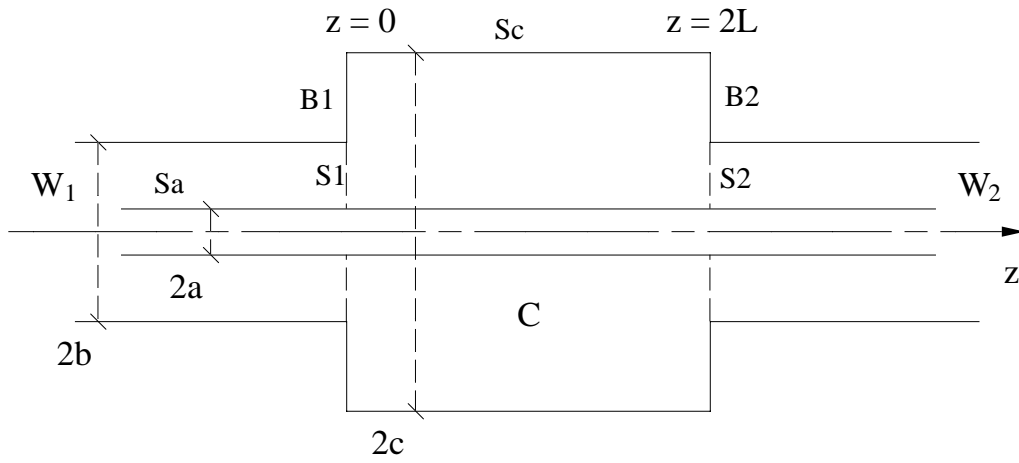


**FIG.1:** geometry of the cavity powered by a circular coaxial waveguide.

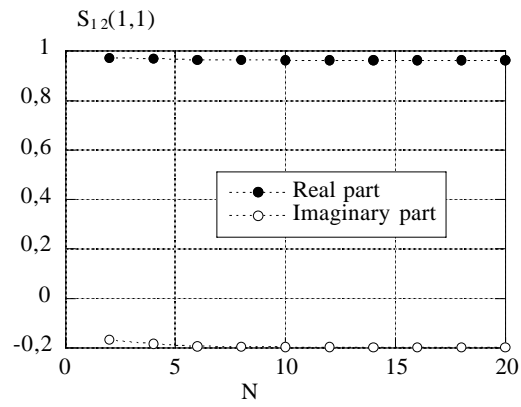
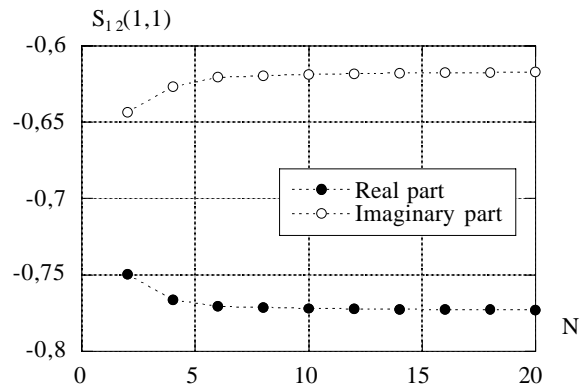


**FIG. 2:** Convergence near a resonant frequency at 1 GHz (a) and at 4 GHz (b).

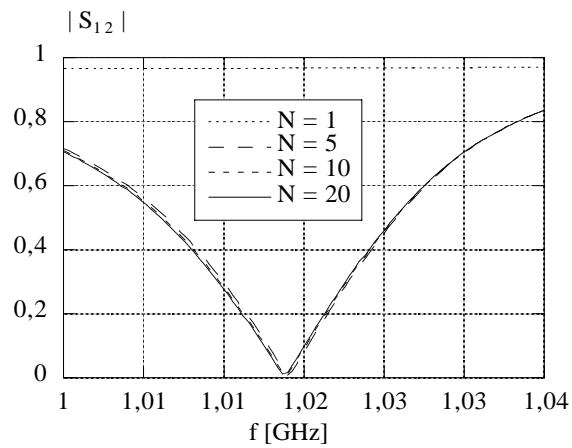


**FIG. 3:** the convergence of the proposed method around the a resonance.

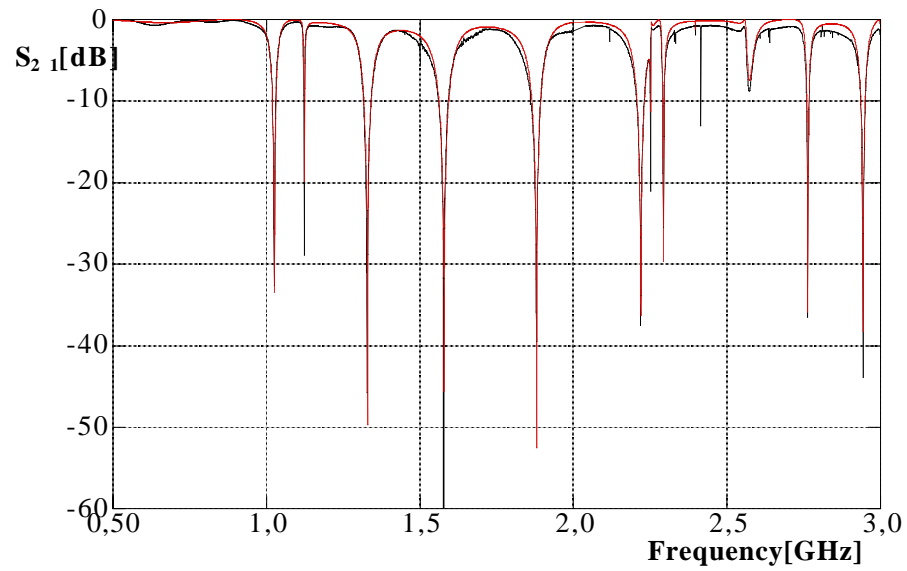


**FIG. 4:** Transmission scattering coefficient: comparison between theory and measurements.

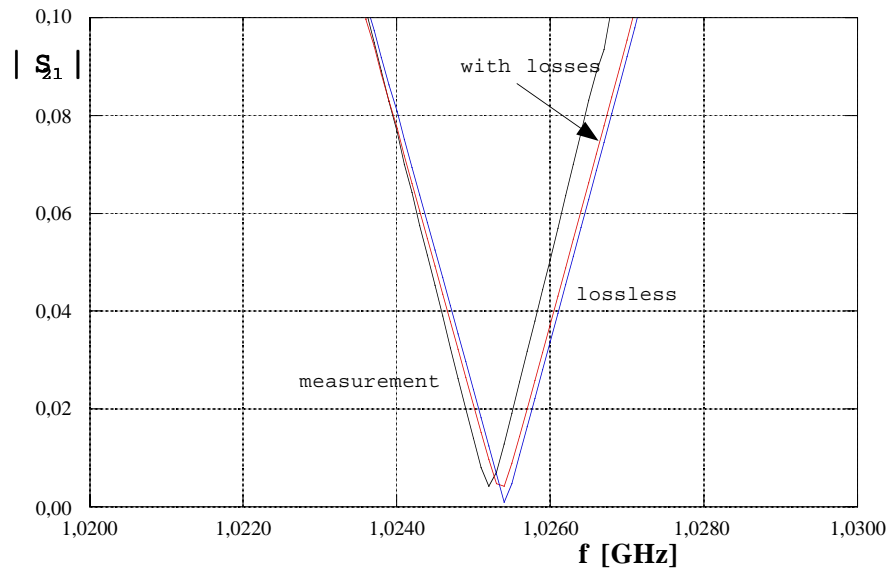


**FIG. 5 :** Pill-box cavity first resonance: comparison between the measured data and the theoretical ones (with and without losses).